Comparative End-to-End Delay Analysis of Repetition and RaptorQ Codes for URLLC in Smart Factory Automation

Athirah Mohd Ramly
Department of Computing and Digital Technologies
School of Architecture, Computing and Engineering
University of East London
London E16 2RD, United Kingdom
a.mohd-ramly@uel.ac.uk

Christopher Laskiewicz de Friedensfeld Bernasiński
Department of Computing and Digital Technologies
School of Architecture, Computing and Engineering
University of East London
London E16 2RD, United Kingdom
u2604779@uel.ac.uk

***Abstract*—Ultra Reliable Low Latency Communication (URLLC) is crucial for industrial factory automation, where stringent delay and reliability requirements must be met. Hence, this paper evaluates the end-to-end delay (E2E) performance of two Forward Error Correction (FEC) techniques such as Repetition codes and RaptorQ codes within a large-scale factory environment. To assess their reliability under challenging conditions, 100 sensors per square kilometer are deployed, and performance is analyzed across two frequency spectrums: 3.5GHz (mid-band) and 28GHz (high band). The results demonstrate that RaptorQ codes consistently meet the strict URLLC latency requirement of 1 ms, outperforming Repetition codes in all scenarios. The results indicate that RaptorQ at 3.5GHz achieved a maximum coverage of 420 meters for end-to-end (E2E) delay under perfect CSI, 380 meters with frequency diversity, and 360 meters under imperfect CSI without frequency diversity. The study further highlights the benefits of RaptorQ's systematic encoding in maintaining low-latency communication, especially in dynamic industrial environments.**

Keywords— URLLC, RaptorQ, Repetition Codes, Industrial Wireless Communication, Forward Error Correction, Low-Latency, Factory Automation

I. INTRODUCTION

A key component of next-generation (5G) networks is machine-to-machine (M2M) communication, which enables a vast number of multipurpose devices to connect with one another without the need for human assistance [1]. While connected, the devices are expected to communicate and transmit packets seamlessly with surrounding objects, making ultra-reliability and low latency essential [2]. In applications such as smart factory, the main challenge is ensuring that packets are transmitted and received in compliance with 5G's stringent requirements.

The fundamental inspiration for this research originates from the appearance of Beyond 5G (B5G), which uses millimeter-wave technology, RaptorQ codes at the APP layer, and technological adjustments to investigate overall system performance at the APP layer by introducing RaptorQ codes. Designing dependable transmissions under demanding situations is an important part of massive machine-type communication (mMTC). As a result, it is critical to investigate and assess signal performance at the APP layer, considering the role of frequency diversity in channel coding. This research focuses on an investigation of signal performance at the APP layer, especially E2E latency, using RaptorQ codes. The results are then compared to Repetitive codes, a sort of fountain code in channel coding in terms of carrier frequencies, sensors movement and the network densities.

The paper is organized as follows: Section II describes the core theory and parameter assumptions behind the system model. Section III analyses the E2E latency at the APP layer. Section IV goes over the results in depth, and Section V closes the study.

II. LITERATURE REVIEW

This section reviews previous works on forward error correction (FEC) in ultra-reliable low-latency communication (URLLC), particularly in industrial environments. While many studies address channel coding at lower layers (PHY and MAC), fewer have considered application-layer techniques such as RaptorQ codes in high-density smart factory settings. Prior research has mostly focused on simpler error correction codes or physical-layer enhancements, leaving a gap in the evaluation of systematic FEC methods for APP-layer URLLC. This paper fills this gap by offering a comprehensive comparative study between Repetition codes and RaptorQ codes across mid-band and high-band frequencies, emphasizing E2E delay and coverage under mobility and channel diversity.

An appropriate multiple access must be put in place to satisfy the demanding standards of 5G. Non-Orthogonal Multiple Access (NOMA) has been recognized as one of the most effective multiple accesses (MA) techniques for meeting the requirements. One of the most popular NOMA techniques is SCMA, or Sparse Code Multiple Access. [3]. SCMA integrates both the Quadrature Amplitude Modulation (QAM) mapper and the symbol spreader into a single SCMA encoder block, enhancing system efficiency.

The Message Passing Algorithm (MPA) is used instead of the traditional Maximum A Posteriori Probability (MAP) detection to make the receiver's computations more efficient by taking use of SCMA's sparsity [4]. For practical implementation and to achieve near-optimal Quality of Service (QoS), SCMA systems must incorporate channel coding techniques. In [5], Polar codes were implemented with a separate detection and decoding scheme. However, the study also demonstrated that this separation is not optimal due to the high computational complexity involved in the receiver processing. Hence, a proper integration of channel coding and SCMA-NOMA must be investigated to bridge the gaps. Meanwhile in Medium Access Control (MAC) layer, dynamic scheduling [6] is considered ideal for applications involving high bandwidth consumption, infrequent transmissions, and bursty signal patterns. Email, web surfing, and internet streaming are some examples. However, it is not ideal for real-time applications like phone conversations or remote operations. To provide high capacity and dependability while preserving efficient control signaling, a semi-permanent scheduling system is desired that incorporates elements of both dynamic and persistent scheduling [7]. Semi-persistent scheduling has two main components: persistent scheduling for initial transmissions and dynamic scheduling for retransmissions.

In APP layer, one solution for achieving seamless packet transmission is the implementation of an appropriate coding scheme [8]. The Luby Transform (LT) code [9] is one of the most popular fountain codes. LT codes developed into Raptor codes, which has been proved to lower decoding complexity and alleviate the high error floor that exists in LT codes [9]. As a result, rateless fountain codes effectively address reliability challenges in massive machine type communication (mMTC) applications. Raptor codes have further evolved into RaptorQ codes, which extend to a higher-order field to enhance their capacity and capability [10]. Subsequently, RaptorQ codes offer a significant advantage by allowing the quantity of redundant symbols to be calculated on the fly, eliminating the need for precise channel information before data transmission. This flexibility makes them highly suitable for multicast and broadcast transmissions, which lack an Automatic Repeat Request (ARQ) mechanism. Instead, the fountain codes technique transmits redundant data alongside the original packets, ensuring that receivers can reconstruct lost or corrupted source data using these additional symbols. This capability enhances reliability and efficiency, particularly in challenging communication environments where packet loss is common, making RaptorQ codes a robust solution for error recovery [11].

To accommodate the challenging environment of a smart factory, where a massive number of devices are deployed and operate simultaneously, a report from [12] provides an overview of radio system usage from an industrial perspective. As highlighted in the report, applications in smart industries must achieve extremely high reliability, with a packet error rate (PER) of 10^{-9} and latency as low as 1 ms. Additionally, the packet size is designed to be no more than 50 bytes, with the goal of fully utilizing fountain codes for efficient transmission using short packets, ensuring seamless and reliable communication in industrial settings [13]. Smart factory concepts rely on real-time data collection from production lines, necessitating efficient wireless communication in harsh manufacturing environments. RaptorQ coding has been presented as a critical facilitator for designing resilient network protocols in such situations. [14]. While previous studies have implemented channel coding and network coding in smart factory settings, using methods such as Random Linear Network Coding, LT codes, Raptor, and RaptorQ, however, none have thoroughly investigated the performance of RaptorQ codes when diversifying coding matrices [15]. This study aims to bridge that gap.

III. SYSTEM DESIGN

A. *Physical (PHY) Layer Model*

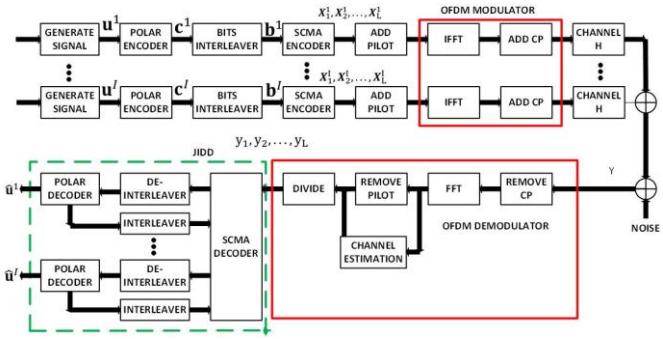

Figure 1 Proposed block diagram at PHY layer

This study simulates a polar-coded SCMA-OFDM system that integrates joint iterative detection and decoding at the receiver. To enhance accuracy, pilot symbols are inserted and minimum mean square error (MMSE) channel estimation is employed to reduce errors at the receiver's end. The overall system block diagram at the PHY layer is illustrated in Figure 1.

Figure 1 depicts the suggested concept for SCMA. B and C represent binary and complex number sets, respectively, whereas x and **X** designate scalar vectors and matrices. Initially, an uplink SCMA system with K users is considered, as shown in Figure 1. The binary bits of the K users, U, are generated as $U = \{u_1, u_2, \ldots, u_i\}$. These information bits are then encoded by a polar encoder into $C = \{c_1, c_2, \ldots, c_i\}$, where i satisfies $1 \le i \le I$.

Subsequently, the uncoded bits are represented as $u^i = \{u_1^i, u_2^i, \ldots, u_m^i\}$, and their corresponding coded bits as $c^i = \{c_1^i, c_2^i, \ldots, c_n^i\}$. Each user's codewords, denoted by $b^1, b^2, \ldots, b^I$, are then interleaved using a random interleaver. The random interleaver plays a crucial role in reducing the correlation between neighboring codeword bits in the polar code, thereby improving the overall system performance. The SCMA encoder maps each $Q = log_2(M)$ bit of b^i to a J-dimensional complex codeword $x^i = \{x_1^i, x_2^i, \ldots, x_j^i\}$. M indicates the constellation size. As a result, $L = N/Q$ represents the entire amount of SCMA codewords. Each codeword contains symbols from I users, but the SCMA codewords include J users. SCMA overloading factor is defined as I/J.

The channel gain matrix between base station and user I on the l-th block is represented as $h_{lj}{}^{i}$, which specifies the channel coefficient vector of user i and resource j at block l. The received symbols at the receiver are then constructed, where $x_l{}^{i} = [x_{l1}{}^{i}, x_{l2}{}^{i}..., x_{lj}{}^{i}]$ denotes the l-th SCMA codeword of user i. Additive White Gaussian Noise (AWGN) is indicated as z_l, with zero mean and unit variance. SCMA multiuser detection is carried out at the receiver before polar decoding begins. This is referred to as the distinct scheme [16], and the Message Passing Algorithm (MPA) is frequently employed for SCMA multiuser detection. Alternative detection methods such as Successive Cancellation (SC) [17], Successive Cancellation List (SCL) [18], Belief Propagation (BP) [19], and the Soft-Cancellation Algorithm (SCAN) can also be used inside the separate scheme [4] for polar decoding.

To effectively use the internal message exchange between the SCMA detector and the JIDD receiver's polar decoder, the system must function as a Single-Input-Single-Output (SISO) system with a different scheme. SCAN has the benefit of requiring less memory and achieving quicker signal convergence while preserving the same cost per iteration as the Belief Propagation method [19]. Table I displays the parameters utilized in the simulation at the PHY layer.

Frequency diversity is done by spreading coded bits among many frequency domain resource blocks, each with its own set of channel constraints. The usual coherence bandwidth in an interior industrial automation setting is 2 to 3 MHz, according to [19]. However, this study suggests a smaller bandwidth of 200 kHz, which considerably improves power efficiency, machine capability, and spectrum usage, benefiting mMTC applications [6]. Furthermore, this research investigates the significance of frequency diversity in enhancing wireless communication reliability in mMTC networks.

TABLE I: SIMULATION PARAMETERS USED AT PHY [5-7]

Parameters	Values
Modulation	SCMA-OFDM
SCMA codewords	4
SCMA codebook size	4
SCMA layers	6
Bandwidth (kHz)	200 (NB-IoT)
Scenario	NLOS Indoor Factory
Subframe time (ms)	1
Channel Model	Rayleigh + AWGN
Receiver type	MMSE
Carrier frequency (GHz)	3.5 / 28
Channel coding	Polar
Code rate	1/2
Channel Estimation	MMSE

The datasets gathered from the simulation at the PHY layer such as Bit Error Rate (BER) and throughputs are then carried forward to the MAC layer for the simulation at network layer.

B. MAC Layer Model

The event-based MATLAB simulator considers a big manufacturing building with dimensions of 20 meters in height, 1,000 meters in width, and 64 meters in length. Six lengthy assembly lines or conveyor belts are created throughout the structure, with 100 devices distributed and spread throughout, as seen in Fig. 2. The simulation includes periodic traffic, and semi-persistent scheduling (SPS) is used because of the latency improvements it provides. SPS optimizes scheduling by using knowledge from prior traffic characteristics, such as inter-arrival time and data size. In this simulation, 100 bits of data packet and 10ms for inter-arrival time are considered. Furthermore, the queue size is supposed to be limitless, allowing it to expand without restriction.

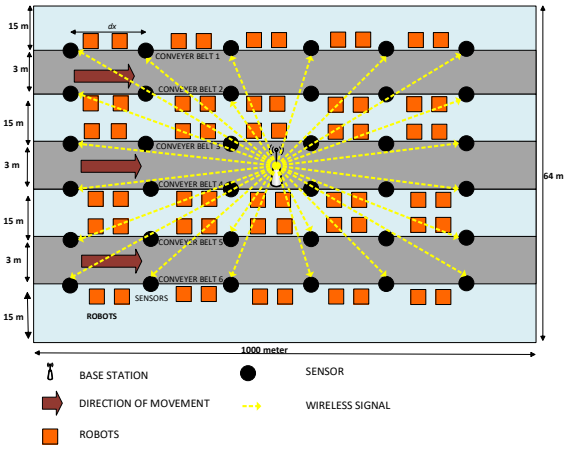

Figure 2 Proposed factory layout settings at MAC layer

Algorithm 1 Semi-Persistent Scheduling at MAC Layer

for $t = 1$ to (current_time / TTI) **do**
  for $j = 1$ to (current_time / ρ) **do**
    M2M sensors di, pi for $i \in [1, M]$
    Determine the Unit Frequency Band (UFB)
    if ($k > k_{\max}$) **then**
      Remove the lowest-priority device from scheduling
    else if ($k < k_{max}$) **then**
      Perform dynamic scheduling for $[k+1, k_{max}]$
    else
      Apply semi-persistent scheduling for $[1, k]$
    end if
    M2M sensors di, pi for $i \in [1, S]$
    Execute call entrance command algorithm
  end for
end for

TABLE II: SIMULATION PARAMETERS AT MAC [3]

Parameters	Values
Traffic Model	Periodic
BS Transmit Power (dBm)	30
Noise Figure (dB)	5
Payload size (bytes)	200
Speeds (for moving robotics) (mph)	0 /10
Number of Lane	6
Lane width(m)	1
Simulation area size (m)	1000 x 64 x 20

Diversity	Frequency
Subcarrier Spacing (kHz)	75
Symbol duration (μs)	13.4
Cyclic Prefix (μs)	0.9 / 3.3 (extended)
Subframe (ms)	0.2
Data rate (kbps)	8.4

This study also considers a first-come-first-served dispatching discipline, an M/G/1 queuing model, and a Poisson distribution for the arrival rate. Another key factor in the simulation is the propagation model. Carrier frequencies of 28GHz and 3.5GHz are analyzed. An obstructed Line-of-Sight (OBS) loss of 9 dB is introduced, as the industrial building contains highly reflective materials such as metals and features a high ceiling and an open layout. The path-loss model for challenging indoor environment, is used to calculate the received power, as in Equation (1) and (2).

$$P_R(s,t) = P_T(s,t) + L_p(s,t) + X_\sigma \quad (1)$$

Where $P_R(s,t)$ represents the received power at location (s,t). $P_T(s,t)$ represents the transmitted power at location (s,t). $L_p(s,t)$ denotes the path loss at (s,t). X_σ represents a random variable.

$$L_p(s,t) = 31.84 + 21.50\log_{10}(d_{s-s}) + 19.00\log_{10}(f_c) \quad (2)$$

$L_{p(s,t)}$ denotes the path loss at position (s,t). d_{s-s} is the distance between the transmitter and receiver, and fc is the carrier frequency. PER and throughput performance are measured in terms of speed, network density, and frequency spectrum. The cross-layer performance of the polar-coded SCMA-OFDM system is evaluated to be over a minimum of 3,000 iterations for each signal-to-noise ratio (SNR) to ensure an accurate representation of the average fading time. The datasets collected from the simulation at the MAC layer, including Packet Error Rate (PER) and throughput, are then forwarded to the APP layer for further analysis.

C. Application (APP) Layer Model

The encoder in RaptorQ constructs a source block by processing incoming User Datagram Protocol (UDP) packets. Each block consists of k symbols, each of which contains T bytes. The encoder then produces N encoded symbols with T bytes per block. Because of RaptorQ's systematic structure, the first k source symbols are included in the N encoded symbols, while the remaining R symbols serve as repair symbols, where $N = k+R$. The code rate (CR) is calculated as $CR = k/N = k/(k+R)$, or $CR=1/\gamma = (1 / 1+\varepsilon)$. Where ε is the Raptor code's overhead. At the receiving end, the RaptorQ decoder waits for all UDP packets corresponding to a given source block to arrive. Decoding begins when the total number of received packets, including source and repair symbols, exceeds $k' = (\varepsilon+1)\, k$. The decoder has a high likelihood of reconstructing the original source block, guaranteeing that all source packets are recovered and transmitted to the APP layer.

In this instance, $CR = 1$ denotes the lack of repair symbols, but $CR = 0.5$ suggests a 50% increase in overhead. This model assumes the UDP protocol has minimal latency and no retransmissions. N_{max} is the greatest number of sensors within a sensing range of $r_{sense} = 100$ from the sending sensor, whereas $N_{receive}$ is the number of sensors that successfully receive the signal from N_{max}. PER_{phy} also indicates the PHY layer's PER, which is determined at the physical layer. End-to-end latency calculations include the overhead associated with the chosen FEC techniques. In Repetition codes, the number of repetitions is set to $N_r = 4$. Raptor codes' Encoding Symbol Identifier (ESI) overhead is calculated as $ESI_{K+\varepsilon} = K / CR$.

TABLE III: SIMULATION PARAMETERS AT APP [15]

Parameters	Values
Generation size, T	1024
Total upper layer header, L	23
Source block length, K	20
Code rate, CR	0.5
Base Station height (gNB), m	10
FEC	RaptorQ/Repetition

This study looks at two FEC methods: repetition codes and RaptorQ codes. Repetition codes are included because of their simplicity and lack of feedback requirements, resulting in low computing complexity. However, despite their ease of execution, repetition codes cause substantial delays and wasteful bandwidth use, making them unsuitable for URLLC applications. Given these restrictions, this study concentrates on systematic RaptorQ codes and evaluates their frequency variety under two conditions: static and 10 mph mobility in an indoor condition. The findings are then compared to those from Repetition codes.

IV. RESULTS AND DISCUSSION

The future factory system's performance is measured in terms of E2E latency in an indoor factory setting. The study analyzes and assesses the performance of Repetition codes and RaptorQ codes based on several criteria including spectrum allocation, speed, and frequency diversity. To ensure uniformity, the sensing range $r_{sense} = R$ is set at 100 meters. In addition, it is assumed that all resources are fully accessible ($\delta = 1$), and all sensors are operated in half-duplex mode. Figure 3 and 4 shows the performance of throughput at PHY layer and packet error rates at MAC layer. The E2E latency and coverage distance results shown in this section are computed as mean values across 3,000 Monte Carlo iterations for each SNR level to ensure statistical stability. However, future versions of this work will include 95% confidence intervals and standard deviation bands in the plots to better illustrate result variability and statistical significance.

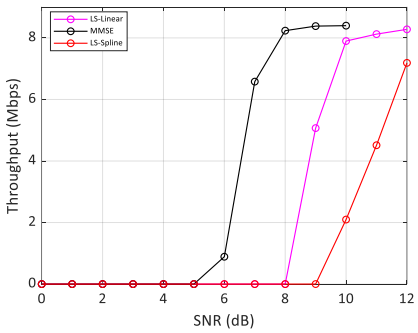

Figure 3 Throughput performance at PHY layer

The E2E delay goal is set at 1 ms to fulfill the URLLC criteria. Figure 5 shows a performance comparison of RaptorQ codes and Repetition codes with perfect Channel State Information (CSI). The findings show that most cases, except for RaptorQ, surpass the 1 ms delay barrier at both the APP and MAC layers. The best performance is achieved with RaptorQ at the APP and MAC layers in a static environment with a high sensor density (dense: 100 sensors per lane per mile) inside the factory landscape. Furthermore, the mid-band spectrum at 3.5GHz exceeds the 28GHz high band spectrum, attaining 420-meter coverage while adhering to the 1 ms delay limit.

Figure 6 depicts a performance comparison of RaptorQ and Repetition codes under frequency diversity. Frequency diversity is done by spreading coded bits over numerous frequency domain resource blocks, each with its own channel coefficients. The best E2E delay performance is observed with RaptorQ codes at both the MAC and APP layers using the 3.5GHz spectrum in a static environment, achieving a total coverage distance of 380 meters within the 1 ms delay constraint. In contrast, the lowest performance is recorded for moving sensors at 10 mph using the 28GHz spectrum, where the total coverage distance within the 1 ms delay, constraint is reduced to 280 meters.

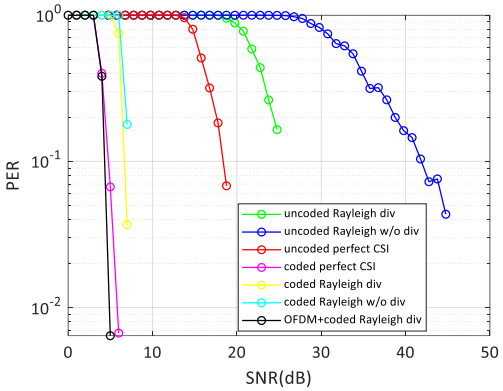

Figure 4 Packet error rates (PER) at MAC layer

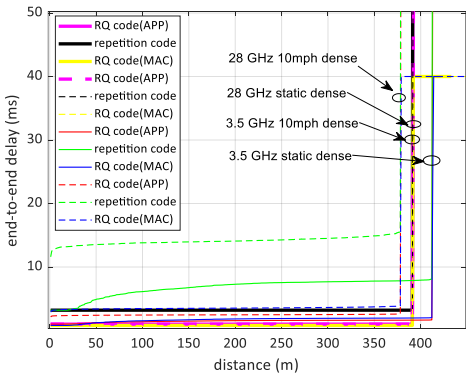

Figure 5 E2E delay at perfect CSI at APP layer

Frequency diversity in resource blocks offers significant benefits at the physical layer of wireless communications. Each resource block experiences unique channel conditions due to factors like multipath fading and interference. By spreading data across different frequency blocks, the system can mitigate the adverse effects of frequency-selective fading. In other words, if one resource block is experiencing a deep fade, other blocks might still provide a reliable channel, thus improving the overall robustness and reliability of the communication link. Additionally, employing frequency diversity allows for more effective use of channel coding and diversity combining techniques, which further enhances error performance and increases throughput.

In Figure 6, frequency diversity is achieved by generating independent channel coefficients for each resource block. In our simulation, the channel coefficients were generated based on a standard fading model, typically Rayleigh fading for non-line-of-sight conditions to capture the variability in each frequency block. Each coefficient is generated independently, implying that there is no inter-block correlation unless specifically modeled otherwise. However, if adjacent resource blocks were to experience correlated fading due to a narrow coherence bandwidth, we would include a correlation factor in the generation process. For the results in Figure 6, we assume that the frequency spacing between resource blocks is sufficiently wide to ensure that the fading coefficients are effectively uncorrelated. This approach allows us to exploit frequency diversity, as any deep fades in one block are unlikely to occur simultaneously in others, thereby enhancing the overall robustness of the communication system.

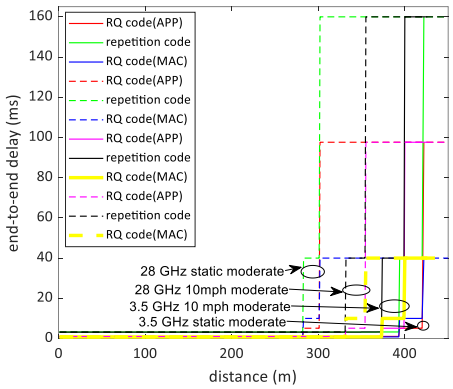

Figure 6 E2E delay with frequency diversity at APP layer

This paper compares the performance of RaptorQ and Repetition codes without frequency diversity, as shown in Figure 7. The absence of frequency diversity results in the lowest overall performance. For static sensors at 3.5 GHz, the end-to-end (E2E) delay coverage reaches 360 meters. In contrast, when sensors are moving at the same frequency, coverage drops to 240 meters. Overall, the mid-band spectrum (3.5 GHz) outperforms the high-band (28 GHz) due to its more stable and robust propagation characteristics, enabling longer and more consistent coverage even during movement. The high-band signal, however, is more susceptible to obstructions, factory clutter, and interference, reducing its reliability in industrial environments.

Static sensors outperform moving ones, as movement introduces Doppler shifts and signal disruptions. Despite this, further study of mobile sensors is important for understanding signal behavior in dynamic conditions. RaptorQ codes emerge as a strong candidate for meeting Ultra-Reliable Low Latency Communications (URLLC) requirements. Their robust source coding makes them

suitable for harsh environments, particularly in indoor industrial settings.

Although RaptorQ offers superior E2E delay and reliability especially with systematic encoding and frequency diversity it has limitations. Its main drawback is the high computational complexity of encoding and decoding, which involves solving systems of linear equations. This can increase latency and energy use, particularly in resource-constrained edge devices. In contrast, Repetition codes are simpler and more efficient for low-power applications. For real-world deployments, future work should focus on optimizing RaptorQ encoding strategies or employing hardware acceleration to address these challenges.

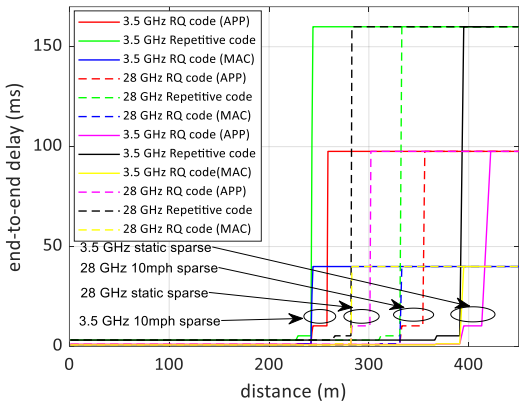

Figure 7 E2E delay without frequency diversity APP layer

A. Limitations and Future Validation

The findings of this study are derived exclusively from simulations conducted across PHY, MAC, and APP layers using standardized models and parameters. While the results convincingly demonstrate RaptorQ's superiority over Repetition codes under various conditions, the absence of real-world testing limits the immediate applicability of the conclusions. Future work should involve hardware-in-the-loop experiments or testbed validation in a real factory setting, using commercial IoT devices and 5G modules, to evaluate practical deployment aspects such as interference, hardware-induced delays, and packet loss due to physical obstructions.

V. CONCLUSION

This paper evaluates E2E delay performance using Repetition and RaptorQ codes in a large-scale factory setting. RaptorQ meets the strict URLLC 1 ms delay requirement in all scenarios and achieves the greatest coverage within this limit, making it ideal for reliable APP-layer transmission. Its systematic encoding enables immediate broadcast of uncoded packets, followed by repair symbols, ensuring low-latency communication. RaptorQ is thus well-suited for URLLC use cases. However, despite its excellent delay performance, further research is needed to assess its computational and energy efficiency, especially for real-time factory deployments in low-power, latency-sensitive environments.

VI. REFERENCES

[1] Huawei, "5G ToB Service Experience Standard Whitepaper", Jan. 2021. [Online] Available: https://carrier.huawei.com/~/media/CNBGV2/download/products/services/5g-b2b-service-experience-standard-white-paper-en1.pdf

[2] S. R. Pokhrel, J. Ding, J. Park, O. -S. Park and J. Choi, "Towards Enabling Critical mMTC: A Review of URLLC Within mMTC," in *IEEE Access*, vol. 8, pp. 131796-131813, 2020.

[3] A. M. Ramly, N. F. Abdullah and R. Nordin, "Cross-Layer Design and Performance Analysis for Ultra-Reliable Factory of the Future Based on 5G Mobile Networks," in *IEEE Access*, vol. 9, pp. 68161-68175, 2021, doi: 10.1109/ACCESS.2021.3078165

[4] Y. Wu, S. Zhang and Y. Chen, "Iterative multiuser receiver in sparse code multiple access systems," 2015 *IEEE International Conference on Communications (ICC)*, London, 2015, pp. 2918-2923.

[5] Z. Pan, E. Li, L. Wen, J. Lei and C. Tang, "Joint *Iterative Detection and Decoding Receiver for Polar Coded SCMA System," 2018 IEEE International Conference on Communications Workshops (ICC Workshops)*, Kansas City, MO, 2018, pp. 1-6.

[6] J. Zhou, X. Zhu, J. Cao and Y. Jiang, "Queue Slicing Based Dynamic Cross-Layer Scheduling for Wireless Deterministic Network with Heterogeneous Traffic," *ICC 2024 - IEEE International Conference on Communications*, Denver, CO, USA, 2024, pp. 5676-5681.

[7] F. Zhang, L. Shan and X. Zhao, "Mathematical Representation for Reliability of Sensing-Based Semi-Persistent Scheduling in LTE-V2X," in *IEEE Transactions on Vehicular Technology*, vol. 71, no. 9, pp. 10115-10119, Sept. 2022, doi: 10.1109/TVT.2022.3176005.

[8] D. Feng, C. She, K. Ying, L. Lai, Z. Hou, T. Q. S. Quek, Y. Li, and B. Vucetic, "Toward ultrareliable low-latency communications: Typical scenarios, possible solutions, and open issues," *IEEE Veh. Technol. Mag.*, vol. 14, no. 2, pp. 94-102, Jun. 2019.

[9] M. Luby, "LT codes," in *Proc. 43rd Annu. IEEE Symp. Found. Comput. Sci*., Vancouver, BC, Canada, Nov. 2002, pp. 271-280.

[10] A. Shokrollahi, "Raptor codes," *IEEE Trans. Inf. Theory*, vol. 52, no. 6, pp. 2551-2567, Jun. 2006.

[11] M. Luby, A. Shokrollahi, M. Watson, and T. Stockhammer, "Raptor forward error correction scheme for object delivery," *Ietf Rmt Working Group Work Prog*., vol. 11, no. 3, pp. 82-89, 2011.

[12] 3GPP TR 45.820 (v13.1.0), "Cellular system support for ultra-low complexity and low throughput Internet of Things (CIoT) (Release 13)," November 2015.

[13] S.-Y. Lien, K.-C. Chen, and Y. Lin, "Toward ubiquitous massive accesses in 3GPP machine-to-machine communications," *IEEE Commun. Mag.*, vol. 49, no. 4, pp. 66–74, 2011.

[14] M., Samokhina, K. Suwon, K., Moklyuk, S., Choi, K., Seoul, & Heo, J."Raptor code-based video multicast over IEEE 802.11 WLAN". In *Proceeding of International Conference Asia Pacific Wireless Communications Symposium*,2008.

[15] A. M. Ramly, N. F. Abdullah and R. Nordin, Application Layer-Forward Error Correction Raptor Q Codes in 5G Mobile Networks for Factory of the Future, *Wireless Communications and Mobile Computing*, 2022, 2257338, 19 pages, 2022. https://doi.org/10.1155/2022/2257338

[16] H. Nikopour and H. Baligh, "Sparse code multiple access," 2013 *IEEE 24th Annual International Symposium on Personal, Indoor, and Mobile Radio Communications (PIMRC)*, London, 2013.

[17] E. Arikan, "Channel Polarization: A Method for Constructing Capacity-Achieving Codes for Symmetric Binary-Input Memoryless Channels," in *IEEE Transactions on Information Theory*, vol. 55, no. 7, pp. 3051-3073, July 2009.

[18] Boutros, E. Viterbo, C. Rastello, and J.-C. Belfiore, "Good lattice constellations for both Rayleigh fading and Gaussian channels," *IEEE Trans. Inf. Theory*, vol. 42, no. 2, pp. 502-518, 1996.

[19] H. Hosseini, A. Anpalagan, K. Raahemifar and S. Erkucuk, "Wavelet-based cognitive SCMA system for mmWave 5G communication networks," *in IET Communications*, vol. 11, no. 6, pp. 831-836, 20 4 2017.